Sensitive MRI markers for systemic amyloidosis: amide proton transfer and equilibrium contrast

A. E. Campbell[1,2], A. N. Price[1,3], S. Walker-Samuel[1], S. Ellmerich[4], P. Simons[4], R. Al-Shawi[4], P. N. Hawkins[4], X. Golay[5], J. C. Moon[6], R. J. Ordidge[2], M. B. Pepys[4], and M. F. Lythgoe[1]

[1]Centre for Advanced Biomedical Imaging, Division of Medicine and Institute of Child Health, University College London, London, United Kingdom, [2]Department of Medical Physics and Bioengineering, University College London, London, United Kingdom, [3]Robert Steiner MRI Unit, Imaging Science Department, Hammersmith Hostpital, Imperial College London, London, United Kingdom, [4]Centre for Amyloidosis and Acute Phase Proteins, Division of Medicine, University College London, London, United Kingdom, [5]Institute of Neurology, University College London, London, United Kingdom, [6]Heart Hospital and Division of Medicine, University College London, London, United Kingdom

Introduction: Systemic amyloidosis is a fatal disorder characterised by the extracellular deposition of insoluble abnormal protein fibrils. Amyloidosis remains a clinical challenge due to difficulties in diagnosis and treatment [1]. To address these challenges, our aim was to develop sensitive MRI markers for the assessment of amyloid accumulation, which could be used to investigate novel treatments in mouse models and provide diagnostically relevant information in the clinical setting.

In this study, two novel MRI techniques were applied to amyloidosis: equilibrium contrast MR (EQ-MR) and amide proton transfer (APT) imaging. EQ-MR relates the volume of distribution (V_d) of gadolinium (Gd), a contrast agent that accumulates in the extracellular matrix, to the expansion of interstitial space in extracellular pathologies such as amyloidosis [2]. APT imaging describes the specific application of chemical exchange saturation transfer (CEST) imaging for detection of amide groups [3], used here for the detection of protein accumulation associated with amyloidosis. Additionally, cine MRI was applied to analyse cardiac function (ejection fraction, stroke volume, left-ventricle mass, etc) [4].

Methods: Ten control and eleven amyloidotic mice, with inducible transgenic over-expression of serum amyloid A protein (SAA) [5], were studied. Imaging was performed on a Varian 9.4T scanner (Varian Inc. Palo Alto, CA, USA) with 35mm coil (RAPID Biomed, Rimpar, Germany).

EQ-MR: A mid-ventricle short-axis slice through the heart, which included a section of liver, was used for EQ-MR. A primed-infusion of Magnevist **(Schering**, Berlin) was used to generate a blood - tissue equilibrium of [Gd]. The dose and timing protocol was optimised empirically such that equilibrium was reached as quickly as possible. A bolus of 0.6mmol/kg was followed 10 minutes later by 0.005mmol/kg/minute infusion of Magnevist. An ECG-gated Look-Locker technique [6] was used to measure the T_1 pre- and post-contrast (TE/TR(inv)/TR(RF)=1.18ms/13.5s/RR-interval, flip=8°, in-plane resolution=200µm, slice thickness=1.5mm). A 3-parameter fit was used to generate T_1 values for regions-of-interest (ROIs) in the myocardium, liver and left ventricle blood pool. The V_d of Gd in the myocardium and liver was calculated using:

$$V_d = (1 - Hct)\frac{\Delta R_{1,tissue}}{\Delta R_{1,blood}}$$

where $R_1 = 1/T_1$ and Hct is the group mean hematocrit, measured from tail-vein blood samples.

APT: APT imaging was applied in the kidney. Axial gradient-echo images (TE/TR = 2.5ms/6s, flip angle = 20°, in-plane resolution = 200µm, slice thickness = 1mm) of the kidney were acquired following RF preparation pulses (100 Gaussian pulses) with top-up saturation pulses between lines of k-space. Preparation pulses of frequencies -3500Hz to +3500Hz in 50Hz steps, corresponding to a range or ±8.75ppm, were used to generate a CEST-spectrum. The magnetisation transfer asymmetry (MTA) was calculated using:

$$MTA\% = \frac{S_{-\omega} - S_{+\omega}}{S_0} \cdot 100\%$$

where S is the signal intensity of the images, with preparation pulses at a frequency indicated by the subscript and S_0 is a reference measurement at a frequency of 80 000Hz. MTA was calculated pixel-wise then averaged for ROIs in the kidney cortex, medulla and pelvis. The %APT was calculated from the mean MTA of the amide proton peak (2.5-4.5ppm) [3]. All image analysis for the EQ-CMR and APT techniques was performed in MATLAB.

Cine MRI: Global cardiac function was calculated from double gated spoiled gradient echo cine images (TE/TR = 1.2/4.5-5ms, cine frames= 20, in-plane resolution=200µm, slice thickness = 1mm, 10 short-axis slices) using the freely available software Segment (http://segment.heiberg.se/).

Figure 1. Comparison of V_d between groups

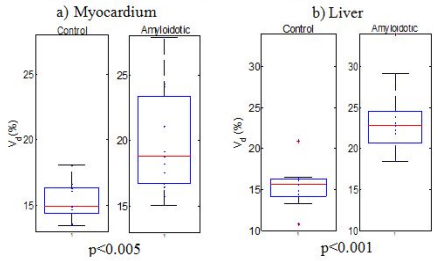

Figure 2. Group mean MTA spectra for the kidney a) cortex, b) medulla, c) pelvis and d) mean of all regions. Standard error of mean is plotted for a selection of data points. The black box represents the amide peak region used to calculate APT (2.5ppm-4.5ppm). Significance between groups (one tail t-test) is shown on each plot.

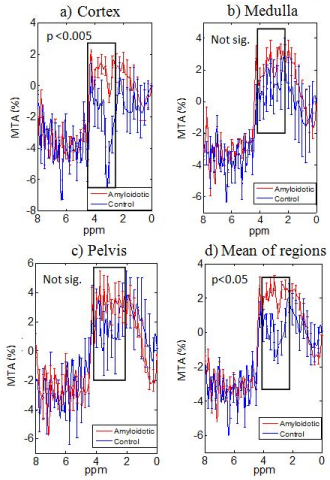

Results: We confirmed by histology that the amyloidotic animals had major amyloid deposits in the liver and minor deposits in their kidneys and heart, as is characteristic of this model [5]. Analysis of cardiac functional parameters calculated from cine images showed no significant difference between the groups. However, using EQ-MR, the amyloidotic group shows a significantly increased V_d of Gd compared to the control group in both organs (Figure 1). The V_d of the control group was 15.4% ± 1.5% (myocardium) and 15.4±2.7% (liver) and of the amyloidotic group 19.8±4.1% (myocardium) and 23.6± 4.6% (liver) (mean ± s.d.). Figure 2 presents MTA spectra of the two groups for the a) cortex, b) medulla c) pelvis and d) mean of kidney regions. The amyloidotic group shows a significant increase in %APT in the kidney cortex (-2.2 ± 2.5% (control) vs. 0.8 ± 1.3% (amyloidotic)), but there was no significant difference in the other regions. Also, a significant difference was observed when the mean of the regions is taken (-0.7 ± 3.1% (control) vs. 1.5 ± 1.5% (amyloidotic)) (mean ± s.d.).

Discussion: In this study, both EQ-MR and APT techniques were able to detect minor amyloid deposits. The EQ-MR procedure has been optimised in the mouse and applied to image the liver and heart. The results of this study show that EQ-MR techniques can detect low levels of amyloid in the heart before impaired cardiac morphology or function can be observed by cine imaging. This approach has the potential to become a sensitive diagnostic tool.

The APT technique has been applied to the kidney and results have indicated the technique's sensitivity to deposition of amyloid. Some technical challenges are introduced when applying CEST techniques to the kidney, due to sensitivity to respiratory motion. It also must be assumed that the fat-content and pH of both groups are the same when applying CEST techniques. The ability to detect the minor deposits in the kidneys indicates that APT imaging may have broad applicability in systemic amyloidosis.

In conclusion, we present two novel MRI techniques for early detection of amyloid deposits. We found that both EQ-MR and APT were useful in detecting minor amyloid deposition, and EQ-MR appeared to be more sensitive than examination of cardiac function. Our results demonstrate that these MRI techniques should be useful for early diagnosis of systemic amyloidosis as well as enable serial quantitative monitoring of response to novel therapies aimed at elimination of amyloid deposits in preclinical studies [7].

References: [1] Pepys MB. *Annu Rev Med* 2006, **57**:223-41. [2] Flett AS et al. *Circulation* 2010, **122**: 138-44. [3] Zhou J et al. *MRM* 2003 **50**: 1120-26. [4] Price AN et al. *Bentham open* 2010, In press. [5] Simons P et al. *Amyloid* April 2010, **17(sl)**: 45-46. [6] Kober F et al. *MRM* 2004, **51**:62-67. [7] Bodin K et al. *Nature* 2010, 268: 93-97.